

University of Groningen

Relativistic two-component formulation of time-dependent current-density functional theory

Romaniello, P.; de Boeij, P. L.

Published in:
Journal of Chemical Physics

DOI:
[10.1063/1.2780146](https://doi.org/10.1063/1.2780146)

IMPORTANT NOTE: You are advised to consult the publisher's version (publisher's PDF) if you wish to cite from it. Please check the document version below.

Document Version
Publisher's PDF, also known as Version of record

Publication date:
2007

[Link to publication in University of Groningen/UMCG research database](#)

Citation for published version (APA):

Romaniello, P., & de Boeij, P. L. (2007). Relativistic two-component formulation of time-dependent current-density functional theory: Application to the linear response of solids. *Journal of Chemical Physics*, 127(17), [174111]. <https://doi.org/10.1063/1.2780146>

Copyright

Other than for strictly personal use, it is not permitted to download or to forward/distribute the text or part of it without the consent of the author(s) and/or copyright holder(s), unless the work is under an open content license (like Creative Commons).

The publication may also be distributed here under the terms of Article 25fa of the Dutch Copyright Act, indicated by the "Taverne" license. More information can be found on the University of Groningen website: <https://www.rug.nl/library/open-access/self-archiving-pure/taverne-amendment>.

Take-down policy

If you believe that this document breaches copyright please contact us providing details, and we will remove access to the work immediately and investigate your claim.

Downloaded from the University of Groningen/UMCG research database (Pure): <http://www.rug.nl/research/portal>. For technical reasons the number of authors shown on this cover page is limited to 10 maximum.

Relativistic two-component formulation of time-dependent current-density functional theory: Application to the linear response of solids

P. Romaniello

Istituto Nazionale per la Fisica della Materia and Dipartimento di Fisica dell'Università di Milano, via Celoria 16, I-20133 Milano, Italy

P. L. de Boei^{a)}

Theoretical Chemistry, Zernike Institute for Advanced Materials, University of Groningen, Nijenborgh 4, 9747 AG Groningen, The Netherlands

(Received 23 February 2007; accepted 14 August 2007; published online 7 November 2007)

In this paper we derive the relativistic two-component formulation of time-dependent current-density-functional theory. To arrive at a two-component current-density formulation we apply a Foldy-Wouthuysen-type transformation to the time-dependent four-component Dirac-Kohn-Sham equations of relativistic density-functional theory. The two-component Hamiltonian is obtained as a regular expansion which is gauge invariant at each order of approximation, and to zeroth order it represents the time-dependent version of the relativistic zeroth order regular Hamiltonian obtained by van Lenthe *et al.*, for the ground state [J. Chem. Phys. **99**, 4597 (1993)]. The corresponding zeroth order regular expression for the density is unchanged, whereas the current-density operator now comprises a paramagnetic, a diamagnetic, and a spin contribution, similar to the Gordon decomposition of the Dirac four current. The zeroth order current density is directly related to the mean velocity corresponding to the zeroth order Hamiltonian. These density and current density operators satisfy the continuity equation. This zeroth order approximation is therefore consistent and physically realistic. By combining this formalism with the formulation of the linear response of solids within time-dependent current-density functional theory [Romaniello and de Boei, Phys. Rev. B **71**, 155108 (2005)], we derive a method that can treat orbital and spin contributions to the response in a unified way. The effect of spin-orbit coupling can now be taken into account. As first test we apply the method to calculate the relativistic effects in the linear response of several metals and nonmetals to a macroscopic electric field. Treatment of spin-orbit coupling yields visible changes in the spectra: a smooth onset of the interband transitions in the absorption spectrum of Au, a sharp onset with peak at about 0.46 eV in the absorption spectrum of W, and a low-frequency doublet structure in the absorption spectra of ZnTe, CdTe, and HgTe in agreement with experimental results. © 2007 American Institute of Physics. [DOI: 10.1063/1.2780146]

I. INTRODUCTION

The growing interest in the new field of spintronics¹ has stimulated impressive progress in the experimental study of spin and charge dynamics as, for example, spin-charge coupling through spin-orbit interaction, nonequilibrium spin population, spin currents, and interaction between the spin of charge carriers and the magnetic properties of materials. Time-dependent current-density-functional theory (TD-CDFT) offers a convenient possibility to treat in a unified way charge and spin dynamics. In order to obtain this a fully relativistic treatment is required that includes spin-orbit interaction. This is possible within quantum electrodynamics, where a relativistic density functional theory can be formulated.^{2–4} This leads to the four-component Dirac-Kohn-Sham (DKS) equations.^{5,6} These equations can describe both electrons and positrons. However, fully relativistic calculations based on a four-component Hamiltonian are not needed in order to describe the coupled charge and spin dynamics.

Furthermore, four-component approaches are, in general, more demanding. Therefore, several two-component formalisms have been developed using the Foldy-Wouthuysen transformation,⁷ as, for example, the well-known Pauli expansion. One of the more elegant approaches is based on the regular approximation.^{8,9} The regularized two-component relativistic Hamiltonian arises from a perturbation expansion for a Foldy-Wouthuysen-type transformation that remains regular, unlike the Pauli expansion (see, e.g., Ref. 10), even for singular attractive Coulomb potentials. The regularization can be obtained by introducing a general unitary transformation similar to the one introduced by Foldy and Wouthuysen, which is then represented as a series expansion, but now using a different expansion parameter. The regularization amounts to a resummation of the original Foldy-Wouthuysen expansion, which is formally equivalent to the original one provided that both expansions converge. In this article we will therefore refer to any unitary transformation of the Dirac Hamiltonian that decouples the electron- and positronlike solutions as a Foldy-Wouthuysen transformation. Next to being

^{a)}Electronic mail: p.l.de.boei@rug.nl

regular, the regularized expansion for the Hamiltonian contains the most important relativistic effects, including spin-orbit coupling, already in the leading order term. These effects are normally introduced only at first order in the Pauli expansion. The regular zeroth order Hamiltonian turns out to be identical to the Hamiltonian derived earlier by Chang *et al.*¹² and Heully *et al.*¹¹ Recently, Wang *et al.* and Peng *et al.* proposed a time-dependent density-functional formalism which makes use of the two-component zeroth order regular approximation and a noncollinear exchange-correlation functional to calculate the excitation energies in molecules.^{13–16} They showed that this relativistic time-dependent density-functional theory (TDDFT) formalism has the correct non-relativistic limit, reproduces the correct threefold degeneracy of the triplet excitations, and yields excitation energies with errors comparable to nonrelativistic TDDFT calculations on light elements. However, at the best of our knowledge, a derivation of the time-dependent zeroth order regular formulation has not been given. In this work we derive the time-dependent relativistic two-component current-density functional formulation in analogy to the derivation for the ground state given by van Lenthe *et al.*⁸ We obtain a method that can treat in a unified way the orbital and spin contributions to the response of a system to an electromagnetic field. A similar formalism that treats scalar relativistic effects only has previously been combined with the time-dependent current-density functional formulation of the linear response of solids to a macroscopic electric field.^{17–19} Although the scalar relativistic effects account for the most important relativistic contributions in the spectra,^{19,20} some characteristic features were still missing due to the neglect of spin-orbit coupling. For example, in the group VB and VIB bcc transition metals the treatment of spin-orbit coupling is expected to yield a finite gap in the interband contribution to the absorption spectra, while in the scalar relativistic calculations the absorption remains finite even down to $\hbar\omega=0$ eV.²⁰ Other examples are the widely studied II-VI semiconductors ZnTe and CdTe and semimetal HgTe in the zinc-blende structure.^{21–30} Here the appearance of a low-frequency doublet structure in the optical spectra is ascribed to spin-orbit coupling.^{22–24} To test our method we calculate the dielectric functions of Au, W, ZnTe, CdTe, and HgTe, and we show that spin-orbit coupling, which has a considerable impact on the electronic structure of these systems, becomes visible in the optical spectra, in particular, for HgTe. The outline of this paper is as follows. In Sec. II we derive the time-dependent relativistic two-component Kohn-Sham Hamiltonian and the corresponding density and current-density operators, and we show their gauge invariance order by order. Next we consider the zeroth order approximation of these expressions, and we combine them with the formulation of the linear response of solids within TDCDFT.^{31–33} In Sec. III we compare our results with available experimental data.^{23–25,28,29,34,35}

II. THEORY

Relativistic density functional theory (RDFT) has been formulated for the ground state within the framework of

quantum electrodynamics, where the renormalization procedure provides a minimum principle, which makes possible the relativistic extension of the Hohenberg-Kohn theorem.² Recent reviews of the quantum electrodynamical basis of RDFT have been given by Engel and Dreizler³ and Engel.⁴ Before proceeding we introduce the following notations: the four-vector event $(x^\mu)=(ct, \mathbf{r})$, the ordinary four-vector derivatives $(\partial_\mu)=(\partial/\partial x^\mu)=(1/c\partial/\partial t, \nabla)$, the four-vector current $(j^\mu)=(c\rho, \mathbf{j})$, and the four-vector external potential $(A^\mu)=(\Phi, \mathbf{A})=(-v, \mathbf{A})$. Throughout the paper we will indicate four-component vectors with the notation (a^μ) , where $\mu=0, 1, 2, 3$ if not indicated otherwise. Furthermore, for a general four-vector (a^μ) , we will use the notation (a_μ) to indicate a four-vector with $a_0=a^0$ and $a_i=-a^i$ ($i=1, 2, 3$). Using the renormalized ground-state energy E_0 and the renormalized ground-state four-current $(j^\mu(\mathbf{r}))$, one can prove that there exists a one-to-one correspondence between the set of four-component external potentials $\{(A^\mu(\mathbf{r}))\}$, just differing by gauge transformations $A^\mu \rightarrow A^\mu - \partial^\mu \Lambda$, the associated set of (nondegenerate) ground-state wave functions $\{\Phi_0\}$, just differing in phase $\Phi_0 \rightarrow \Phi_0 e^{-i\Lambda/c}$, and the ground-state four-current $(j^\mu(\mathbf{r}))$ of the system.^{3,4} This means that the ground-state wave function is, apart from the gauge freedom, a unique (and universal) functional of the ground-state four current. As consequence, the ground-state energy of the system is a universal functional of the ground-state current. The exact $(j^\mu(\mathbf{r}))$ minimizes $E_0[j]$ under the constraint of charge conservation,

$$\sum_{\mu} \partial_{\mu} j^{\mu}(\mathbf{r}) = 0. \quad (1)$$

In order to derive the relativistic Kohn-Sham equations,^{5,6} one has to assume the possibility to reproduce the exact ground-state four current of the interacting system in an auxiliary system of noninteracting particles in effective potentials $(A_s^\mu(\mathbf{r}))$. We expect that statements analogous to the nonrelativistic case also hold in the relativistic description. Within the relativistic Kohn-Sham scheme, the ground-state four current can be represented in terms of auxiliary single-particle four spinors Ψ_i , which are solution of the following Dirac-Kohn-Sham equation:^{3,4}

$$\{c\boldsymbol{\alpha} \cdot \boldsymbol{\pi} + \beta c^2 + v_s(\mathbf{r})\}\Psi_i(\mathbf{r}) = \epsilon_i \Psi_i(\mathbf{r}), \quad (2)$$

where $\boldsymbol{\pi} = \mathbf{p} + \mathbf{A}_s(\mathbf{r})/c$ and β is the four-by-four matrix,

$$\beta = \begin{pmatrix} I & 0 \\ 0 & -I \end{pmatrix}, \quad (3)$$

with I the two-by-two identity matrix. We also define the four-component velocity operator $\alpha^\mu = (\alpha^0, \boldsymbol{\alpha})$ with α^0 the four-by-four identity matrix and

$$\boldsymbol{\alpha} = \begin{pmatrix} 0 & \boldsymbol{\sigma} \\ \boldsymbol{\sigma} & 0 \end{pmatrix}. \quad (4)$$

Here $\boldsymbol{\sigma}$ is the vector of two-by-two Pauli matrices,

$$\sigma_x = \begin{pmatrix} 0 & 1 \\ 1 & 0 \end{pmatrix}, \quad \sigma_y = \begin{pmatrix} 0 & -i \\ i & 0 \end{pmatrix}, \quad \sigma_z = \begin{pmatrix} 1 & 0 \\ 0 & -1 \end{pmatrix}. \quad (5)$$

This single-particle description, in general, also includes vacuum polarization contributions.^{3,4} However, for most RDFT applications these electrodynamic effects can be neglected (the so-called no-pair approximation), which we will do in the sequel. The renormalized ground-state four current can then be expressed as

$$j^\mu(\mathbf{r}) = c \sum_{-c^2 < \epsilon_i \leq \epsilon_F} \Psi_i^\dagger(\mathbf{r}) \alpha^\mu \Psi_i(\mathbf{r}), \quad (6)$$

where ϵ_F is the Fermi level of the auxiliary system and the summation is over the occupied electronic states. The Kohn-Sham four potential $(A_s^\mu(\mathbf{r})) = (-v_s(\mathbf{r}), \mathbf{A}_s(\mathbf{r}))$ consists of the external, the Hartree, and the exchange-correlation four potentials, respectively,

$$v_s(\mathbf{r}) = v_{\text{ext}}(\mathbf{r}) + \int d\mathbf{r}' \frac{\rho(\mathbf{r}')}{|\mathbf{r} - \mathbf{r}'|} + v_{\text{xc}}(\mathbf{r}), \quad (7)$$

$$\mathbf{A}_s(\mathbf{r}) = \mathbf{A}_{\text{ext}}(\mathbf{r}) + \frac{1}{c} \int d\mathbf{r}' \frac{\mathbf{j}_T(\mathbf{r}')}{|\mathbf{r} - \mathbf{r}'|} + \mathbf{A}_{\text{xc}}(\mathbf{r}), \quad (8)$$

where $\mathbf{j}_T(\mathbf{r}')$ is the transverse current density.³⁶ Here the exchange-correlation four potential $(\mathbf{A}_{\text{xc}}^\mu(\mathbf{r})) = (-v_{\text{xc}}(\mathbf{r}), \mathbf{A}_{\text{xc}}(\mathbf{r}))$ is defined by the relation

$$\lim_{\lambda \rightarrow 0} \frac{E_{\text{xc}}[j^\mu + \lambda \delta j^\mu] - E_{\text{xc}}[j^\mu]}{\lambda} = - \int A_{\text{xc},\mu}(\mathbf{r}) \delta j^\mu(\mathbf{r}) d\mathbf{r} \quad (9)$$

for any δj^μ such that $j^\mu + \lambda \delta j^\mu$ belongs to the set of real currents on which $E_{\text{xc}}[j^\mu]$ is defined. Here $A_{\text{xc},\mu}(\mathbf{r})$ is determined up to a gauge transformation $A_{\text{xc},\mu}(\mathbf{r}) \rightarrow A_{\text{xc},\mu}(\mathbf{r}) + \partial_\mu \Lambda_{\text{xc}}(\mathbf{r})$ as

$$\int \partial_\mu \Lambda_{\text{xc}}(\mathbf{r}) j^\mu(\mathbf{r}) d\mathbf{r} = - \int \Lambda_{\text{xc}}(\mathbf{r}) (\partial_\mu j^\mu(\mathbf{r})) d\mathbf{r} = 0, \quad (10)$$

where we have used condition (1). Solution of Eq. (2) leads to four-component wave functions or spinors. The Dirac equation admits both positive energy solutions, associated with electrons, and negative energy solutions, associated with positrons. Normally one is interested in the electronic states only. If the rest mass energy for positive energy states is subtracted by a change of gauge, then the solutions of interest of the Dirac equation are those in which the upper two-component spinor of the wave function is predominant. This component is called large component, while the lower two-component spinor is called small component. The electron and positron states can be completely decoupled by means of unitary transformations, as, for example, the Foldy-Wouthuysen transformation.⁷ The electronic states are then described by a two-component spinor and Hamiltonian. We will not show this here for the ground state, but we will demonstrate it for the time-dependent case, which is the subject of the next section.

A. Time-dependent relativistic two-component formalism

For our derivation of a time-dependent relativistic two-component formalism, we will start from the extension of Eq. (2) to the time domain,³⁷

$$\{c\boldsymbol{\alpha} \cdot \boldsymbol{\pi} + \beta c^2 + v_s(\mathbf{r}, t)\} \Psi_i(\mathbf{r}, t) = i \partial_t \Psi_i(\mathbf{r}, t), \quad (11)$$

with $\boldsymbol{\pi} = \mathbf{p} + \mathbf{A}_s(\mathbf{r}, t)/c$ and where we have used the notation $\partial_t = \partial/\partial t$. The four-component current ($j^\mu(\mathbf{r}, t)$) is now time dependent and it is given by

$$j^\mu(\mathbf{r}, t) = c \sum_i \Psi_i^*(\mathbf{r}, t) \alpha^\mu \Psi_i(\mathbf{r}, t), \quad (12)$$

where the summation is over states which represent the evolution of the initial occupied electronic states of Eq. (2). The scalar component of the four current is the density,

$$\rho(\mathbf{r}, t) = j^0(\mathbf{r}, t)/c = \sum_i \Psi_i^*(\mathbf{r}, t) \Psi_i(\mathbf{r}, t), \quad (13)$$

whereas the vector component is

$$\mathbf{j}(\mathbf{r}, t) = c \sum_i \Psi_i^*(\mathbf{r}, t) \boldsymbol{\alpha} \Psi_i(\mathbf{r}, t). \quad (14)$$

The density $\rho(\mathbf{r}, t)$ and the current density $\mathbf{j}(\mathbf{r}, t)$ satisfy the continuity equation and uniquely determine the external potentials $v_s(\mathbf{r}, t)$ and $\mathbf{A}_s(\mathbf{r}, t)$ as result of the relativistic extension of the Runge-Gross theorem.³⁷

1. Time-dependent relativistic two-component Hamiltonian

Several two-component formalisms have been developed to treat electronic states only. One of the simplest and most elegant approaches is the method of the regular approximation of the Foldy-Wouthuysen transformation. The two-component regular Hamiltonian has already been derived by van Lenthe *et al.* for the stationary case.^{8,9} By following this formulation we will derive here the time-dependent two-component equations by starting from the time-dependent single-particle Dirac-Kohn-Sham equation. The time-dependent DKS equation for the four-component Dirac wave function,

$$\Psi^D(\mathbf{r}, t) = e^{-ic^2 t} \begin{pmatrix} \psi_L(\mathbf{r}, t) \\ \psi_S(\mathbf{r}, t) \end{pmatrix}, \quad (15)$$

can be rewritten in terms of the large and small components ψ_L and ψ_S , respectively,

$$v_s \psi_L + c \boldsymbol{\sigma} \cdot \boldsymbol{\pi} \psi_S = i \partial_t \psi_L, \quad (16)$$

$$c \boldsymbol{\sigma} \cdot \boldsymbol{\pi} \psi_L + (v_s - 2c^2) \psi_S = i \partial_t \psi_S. \quad (17)$$

Similar to the stationary case, a time-dependent two-component relativistic Hamiltonian for electronic states can be generated by finding a unitary transformation U , with $U^{-1} = U^\dagger$, that reduces the time-dependent Dirac Hamiltonian to block diagonal form. In general, U will depend on time. Foldy and Wouthuysen introduced a systematic method for progressively decoupling large and small components.⁷ The transformed Dirac equation is then given by

$$(U\hat{H}^D U^{-1} - U[i\partial_t, U^{-1}])(U\Psi^D(\mathbf{r}, t)) = i\partial_t(U\Psi^D(\mathbf{r}, t)), \quad (18)$$

where \hat{H}^D is the Dirac Hamiltonian defined in Eqs. (16) and (17). This defines the Schrödinger picture where the transformed Hamiltonian \hat{H}^S is given by

$$\hat{H}^S = U\hat{H}^D U^{-1} - U[i\partial_t, U^{-1}], \quad (19)$$

and the corresponding wave function by $\Phi^S = U\Psi^D$. For electronic states Φ^S can be written as

$$\Phi^S = \begin{pmatrix} \phi \\ 0 \end{pmatrix} = U e^{-ic^2 t} \begin{pmatrix} \psi_L \\ \psi_S \end{pmatrix}. \quad (20)$$

The unitary matrix U can be given in terms of an operator \hat{X} as¹¹

$$U = \begin{pmatrix} 1/\sqrt{1 + \hat{X}^\dagger \hat{X}} & (1/\sqrt{1 + \hat{X}^\dagger \hat{X}})\hat{X}^\dagger \\ -(1/\sqrt{1 + \hat{X}\hat{X}^\dagger})\hat{X} & (1/\sqrt{1 + \hat{X}\hat{X}^\dagger}) \end{pmatrix} e^{ic^2 t}, \quad (21)$$

so that,

$$\phi = (1 + \hat{X}^\dagger \hat{X})^{-1/2} (\psi_L + \hat{X}^\dagger \psi_S), \quad (22)$$

$$0 = (1 + \hat{X}\hat{X}^\dagger)^{-1/2} (\hat{X}\psi_L - \psi_S). \quad (23)$$

Here the operator \hat{X} is implicitly time dependent. The last equation is an identity if the operator \hat{X} satisfies the relation

$$\psi_S = \hat{X}\psi_L, \quad (24)$$

for all electronlike states. It then follows that

$$\phi = \sqrt{1 + \hat{X}^\dagger \hat{X}} \psi_L. \quad (25)$$

In the following we will indicate as Schrödinger wave function and Hamiltonian the two-component wave function ϕ and the upper-left part \hat{h}^S of the transformed Dirac Hamiltonian, respectively. We can now formulate equations of motion for ϕ and for \hat{X} . We start by eliminating ψ_S : inserting Eq. (24) in Eqs. (16) and (17) gives the intermediate relations

$$(v_s + c\boldsymbol{\sigma} \cdot \boldsymbol{\pi} \hat{X})\psi_L = i\partial_t \psi_L, \quad (26)$$

$$(c\boldsymbol{\sigma} \cdot \boldsymbol{\pi} + (v_s - 2c^2)\hat{X})\psi_L = [i\partial_t, \hat{X}]\psi_L + i\hat{X}\partial_t \psi_L. \quad (27)$$

From Eqs. (25) and (26) one readily derives the equation of motion for the two-component wave function ϕ ,

$$\hat{h}^S \phi = i\partial_t \phi, \quad (28)$$

in which the two-component time-dependent Hamiltonian \hat{h}^S is given by the upper-left part of the transformed Hamiltonian \hat{H}^S ,

$$\begin{aligned} \hat{h}^S = & v_s + c\boldsymbol{\sigma} \cdot \boldsymbol{\pi} \hat{X} + [i\partial_t - v_s - c\boldsymbol{\sigma} \cdot \boldsymbol{\pi} \hat{X}, \sqrt{1 + \hat{X}^\dagger \hat{X}}] \\ & \times \frac{1}{\sqrt{1 + \hat{X}^\dagger \hat{X}}}. \end{aligned} \quad (29)$$

By combining Eqs. (26) and (27), we obtain the following relation:

$$(c\boldsymbol{\sigma} \cdot \boldsymbol{\pi} + [v_s - i\partial_t, \hat{X}] - 2c^2\hat{X} - \hat{X}c\boldsymbol{\sigma} \cdot \boldsymbol{\pi} \hat{X})\psi_L = 0, \quad (30)$$

which should hold for all electronlike states ψ_L , and therefore it represents an equation of motion for \hat{X} . For the stationary case various approaches to solve this operator equation have been developed and they have recently been analyzed and reviewed by Kutzelnigg and Liu.³⁸ To solve this equation in the time-dependent case we isolate a part $(v_0 - \epsilon) < 2c^2$, with for the moment v_0 an arbitrary function of \mathbf{r} and t and ϵ an arbitrary function of t , so that we can rewrite

$$\hat{X} = (2c^2 - v_0 + \epsilon)^{-1} (c\boldsymbol{\sigma} \cdot \boldsymbol{\pi} + \Xi(\hat{X})), \quad (31)$$

where we introduce the operator Ξ as function of \hat{X} ,

$$\Xi(\hat{X}) = [v_s - v_0 + \epsilon - i\partial_t, \hat{X}] - \hat{X}(v_0 - \epsilon + c\boldsymbol{\sigma} \cdot \boldsymbol{\pi} \hat{X}). \quad (32)$$

We can choose $(v_0 - \epsilon)$ in such a way that the result of $\Xi(\hat{X})$ acting on ψ_L is small for electronlike states, which becomes clear from the relation

$$\Xi(\hat{X})\psi_L = (v_s - v_0 + \epsilon - i\partial_t)\psi_S. \quad (33)$$

The latter relation follows immediately from Eqs. (26) and (32). For example, we can choose v_0 such that $(v_s - v_0)$ is always small everywhere and ϵ is close to the orbital energies of the relevant states. In this way Eq. (31) can be solved by iteration where $\hat{X} = \lim_{n \rightarrow \infty} \hat{X}_n$, with

$$\hat{X}_n = (2c^2 - v_0 + \epsilon)^{-1} (c\boldsymbol{\sigma} \cdot \boldsymbol{\pi} + \Xi(\hat{X}_{n-1})), \quad (34)$$

and an approximate initial choice \hat{X}_{-1} . We must observe that to obtain Eq. (33) we used the relation $\hat{X}\psi_L = \psi_S$, where ψ_L and ψ_S are assumed to be the known exact solutions of the Dirac equation. This relation is, in general, not valid for an approximate solution \hat{X} of Eq. (31). Therefore solving Eq. (31) by iteration is not guaranteed to converge for any given initial trial value of \hat{X}_{-1} . Moreover, the justification of this expansion may become questionable when \hat{X} is acting on electronlike states with high-energy orbital components or if one considers the region near the nuclei, where the small component of the Dirac wave function is not necessarily small. However, this does not rule out that a well-behaved solution for \hat{X} does exist, and that it is well approximated by the few lowest orders of the expansion. We will apply our expansion only at zeroth order, and we do not proceed to higher orders in the present work. It is important to note that, if converging, the term $\hat{X} = \hat{X}_\infty$ does not depend on the particular choice of $(v_0 - \epsilon)$. Moreover, from Eq. (24) it follows that \hat{X} should be gauge invariant as ψ_L and ψ_S refer to solutions of the Dirac equation, which is itself gauge invariant.

For gauge invariance of an operator $\hat{O}[\mathbf{A}_s^\mu]$, which depends on the four-potential \mathbf{A}_s^μ , is meant that

$$e^{i\Lambda(\mathbf{r},t)}\hat{O}[\mathbf{A}_s^\mu(\mathbf{r},t) - \partial^\mu\Lambda(\mathbf{r},t)]e^{-i\Lambda(\mathbf{r},t)} = \hat{O}[\mathbf{A}_s^\mu], \quad (35)$$

where $\Lambda(\mathbf{r},t)$ is an arbitrary scalar function of space and time. As examples the operators $c\boldsymbol{\sigma}\cdot\boldsymbol{\pi}$ and $(v_s - i\partial_t)$ are gauge invariant, and $\Xi(\hat{X})$ is gauge invariant if \hat{X} and $(v_0 - \epsilon)$ are. Thus the iteration retains the gauge invariance of the operator \hat{X} , i.e., \hat{X}_n is gauge invariant if the initial value \hat{X}_0 and $(v_0 - \epsilon)$ are gauge invariant. If we start the iteration by taking $\hat{X}_{-1}=0$, then \hat{X}_0 is similar to the operator used in the stationary case,

$$\hat{X}_0 = (2c^2 - v_0 + \epsilon)^{-1}c\boldsymbol{\sigma}\cdot\boldsymbol{\pi}, \quad (36)$$

with the main difference being that v_0 , ϵ , and $\boldsymbol{\pi}$ may depend on time. If the solution for the operator \hat{X} is truncated at a finite number of iterations, then the results will depend on the particular choice of $(v_0 - \epsilon)$. In practical applications one can demand the potential in the ground state, when calculated in the Coulomb gauge, to vanish at infinity.⁹ In this case, to keep contact with the ground-state zeroth order regular approximation (ZORA) formulation, one can choose $v_0(\mathbf{r})$ stationary and equal to this ground-state potential, and $\epsilon=0$. This fixes $(v_0 - \epsilon)$, but leaves the gauge of $\mathbf{A}_s^\mu(\mathbf{r},t)$ unspecified. This choice will facilitate the discussion of the linear response of solids. The operator \hat{X}_0 as given in Eq. (36) then takes the form of the operator in the zeroth order approximation used in the stationary case.

Using the solution of the equation of motion for \hat{X} , we can now obtain the Hamiltonian in the Schrödinger picture. For this we need to evaluate the commutator in Eq. (29). We express the square root $\sqrt{1 + \hat{X}^\dagger\hat{X}}$ as a Taylor series expansion $\sum_{n=0}^{\infty} a_n (\hat{X}^\dagger\hat{X})^n$, where $a_0=1$, $a_1=1/2$, and $a_n = (-1)^{n-1}(2n-3)!!/(2^n n!)$ for $n > 1$. Using $[A, B^n] = \sum_{m=0}^{n-1} B^{n-m-1}[A, B]B^m$ for $n > 0$, and

$$[i\partial_t - v_s - c\boldsymbol{\sigma}\cdot\boldsymbol{\pi}\hat{X}, \hat{X}^\dagger\hat{X}] = (\hat{X}^\dagger c\boldsymbol{\sigma}\cdot\boldsymbol{\pi} - c\boldsymbol{\sigma}\cdot\boldsymbol{\pi}\hat{X})(1 + \hat{X}^\dagger\hat{X}), \quad (37)$$

which follows from the equation of motion for \hat{X} , Eq. (30), we can express the time-dependent two-component Schrödinger Hamiltonian [Eq. (29)] as

$$\hat{h}^S = v_s + \frac{1}{2}(c\boldsymbol{\sigma}\cdot\boldsymbol{\pi}\hat{X} + \hat{X}^\dagger c\boldsymbol{\sigma}\cdot\boldsymbol{\pi}) + \hat{Y}[\hat{X}], \quad (38)$$

where the operator \hat{Y} can be expressed as

$$\hat{Y}[\hat{X}] = \sum_{p,q} c_{pq} (\hat{X}^\dagger\hat{X})^p (\hat{X}^\dagger c\boldsymbol{\sigma}\cdot\boldsymbol{\pi} - c\boldsymbol{\sigma}\cdot\boldsymbol{\pi}\hat{X}) (\hat{X}^\dagger\hat{X})^q.$$

In Appendix A we show that $c_{pq} = -c_{qp}$, and thus \hat{Y} is Hermitian and, as $c_{00}=0$, of first order in $(\hat{X}^\dagger\hat{X})$. Furthermore \hat{Y} , and thus also the Hamiltonian [Eq. (38)], inherits the gauge invariance of \hat{X} order by order in $(\hat{X}^\dagger\hat{X})$. This allows for physical acceptable approximations by truncating the expansion of \hat{Y} to some order in $n=p+q$. Note that we make use of two series expansions, one for \hat{X} and one for \hat{Y} . Each of them

can be truncated without affecting the hermiticity or the gauge invariance. However, when the expansion for \hat{X} is truncated at finite order, a dependence on the particular choice for $(v_0 - \epsilon)$ remains.

2. Relativistic density and current-density operators

The unitary transformation that is used to reduce the four-component Dirac equation to an effective two-component description represents a picture change: we pass from the Dirac picture to a new picture, which is appropriately called Schrödinger picture. This picture change requires that not only the wave function but also the operators are transformed in order to keep the physics unaltered. For example, the position operator $\hat{\mathbf{r}}$ represents in the new picture a new physical observable which is called the mean position or mass position $\hat{\mathbf{r}}_{\text{mass}}$ of the electron,^{7,39} while the transformed operator $U\hat{\mathbf{r}}U^{-1}$ represents the original position in the new picture. For a generic operator with representation \hat{O}^D in the Dirac picture we can write the Heisenberg equation of motion,

$$\left(\frac{d\hat{O}}{dt}\right)^D = -i[\hat{O}^D, \hat{H}^D - i\partial_t]. \quad (39)$$

Then for the representation \hat{O}^S of the same operator in the Schrödinger picture we have

$$\begin{aligned} \left(\frac{d\hat{O}}{dt}\right)^S &= U\left(\frac{d\hat{O}}{dt}\right)^D U^{-1} \\ &= -i[U\hat{O}^D U^{-1}, U\hat{H}^D U^{-1} - iU\partial_t U^{-1}] \end{aligned} \quad (40)$$

$$= -i[\hat{O}^S, \hat{H}^S - i\partial_t]. \quad (41)$$

Neglecting the picture change results in an error, which is usually small but, for instance, visible for core states.⁴⁰ The single-particle four-current operator is defined in the Dirac picture as

$$\hat{j}^{\mu,D}(\mathbf{r}') = c\delta(\mathbf{r}' - \mathbf{r})\alpha^\mu, \quad (42)$$

where the scalar component gives the single-particle density operator $\hat{\rho}^D(\mathbf{r}') = \delta(\mathbf{r}' - \mathbf{r})\alpha^0$ and the vector component the single-particle current operator $\hat{\mathbf{j}}^D(\mathbf{r}') = c\delta(\mathbf{r}' - \mathbf{r})\boldsymbol{\alpha}$. If we transform $\hat{\rho}^D(\mathbf{r}')$, the two-component Schrödinger density operator $\hat{\rho}^S(\mathbf{r}',t)$ becomes given by

$$\hat{\rho}^S(\mathbf{r}',t) = \frac{1}{\sqrt{1 + \hat{X}^\dagger\hat{X}}}(\delta(\mathbf{r}' - \mathbf{r}) + \hat{X}^\dagger\delta(\mathbf{r}' - \mathbf{r})\hat{X})\frac{1}{\sqrt{1 + \hat{X}^\dagger\hat{X}}}. \quad (43)$$

For the transformed current operator we proceed in a similar way, and the two-component Schrödinger current operator $\hat{j}_\mu^S(\mathbf{r}',t)$ is given by

$$\begin{aligned} \hat{j}_\mu^S(\mathbf{r}',t) &= \frac{1}{\sqrt{1 + \hat{X}^\dagger\hat{X}}}(c\delta(\mathbf{r}' - \mathbf{r})\sigma_\mu\hat{X} \\ &\quad + c\hat{X}^\dagger\delta(\mathbf{r}' - \mathbf{r})\sigma_\mu)\frac{1}{\sqrt{1 + \hat{X}^\dagger\hat{X}}}. \end{aligned} \quad (44)$$

B. Zeroth order regular approximation

We define our zeroth order approximation for the operator \hat{X} by neglecting the term $\Xi(\hat{X})$ in expression (31). Then $\hat{X}=\hat{X}_0$ as given in Eq. (36). It immediately follows from the hermiticity of $\boldsymbol{\sigma} \cdot \boldsymbol{\pi} \hat{X}_0$ that \hat{Y} reduces to zero for this choice of \hat{X} . Using this approximation in Eq. (38) we obtain the time-dependent ZORA Hamiltonian,

$$\hat{h}^{\text{ZORA}}(\mathbf{r}, t) = v_s(\mathbf{r}, t) + \boldsymbol{\sigma} \cdot \boldsymbol{\pi}(\mathbf{r}, t) \frac{c^2}{2c^2 - v_0(\mathbf{r})} \boldsymbol{\sigma} \cdot \boldsymbol{\pi}(\mathbf{r}, t), \quad (45)$$

in which we made the particular choice $v_0(\mathbf{r})$ stationary and equal to the ground-state potential calculated in the Coulomb gauge and vanishing at infinity, and $\epsilon=0$. In a similar way we can obtain the zeroth order expressions for the density and current-density operators. If we take the operator \hat{X} to be the ZORA operator \hat{X}_0 and we neglect in addition terms of the order of $\hat{X}^\dagger \hat{X}$ and higher in Eq. (43), the approximate one-electron ZORA density operator is simply

$$\hat{\rho}^{\text{ZORA}}(\mathbf{r}') = \delta(\mathbf{r}' - \mathbf{r}). \quad (46)$$

This amounts to neglecting the picture change for the density operator, in line with van Lenthe *et al.*,⁹ who showed that the approximate ZORA density reproduces very well the Dirac density, in particular, for the valence region.

Neglecting terms of the order of $\hat{X}^\dagger \hat{X}$ and higher and inserting $\hat{X}=\hat{X}_0$ in Eq. (44), we arrive at the one-electron ZORA current operator,

$$\hat{\mathbf{j}}^{\text{ZORA}}(\mathbf{r}', t) = \left(\delta(\mathbf{r}' - \mathbf{r}) \boldsymbol{\sigma} \frac{K(\mathbf{r})}{2} (\boldsymbol{\sigma} \cdot \boldsymbol{\pi}) + (\boldsymbol{\sigma} \cdot \boldsymbol{\pi}) \frac{K(\mathbf{r})}{2} \delta(\mathbf{r}' - \mathbf{r}) \boldsymbol{\sigma} \right), \quad (47)$$

where $K(\mathbf{r}) = (1 - v_0(\mathbf{r})/2c^2)^{-1}$. By exploiting the property of the Pauli matrices, $\sigma_\mu \sigma_\nu = \delta_{\mu\nu} + i \sum_\tau \epsilon_{\mu\nu\tau} \sigma_\tau$, this expression can be rearranged as

$$\hat{\mathbf{j}}^{\text{ZORA}}(\mathbf{r}', t) = \hat{\mathbf{j}}_p^{\text{ZORA}}(\mathbf{r}', t) + \hat{\mathbf{j}}_d^{\text{ZORA}}(\mathbf{r}', t) + \hat{\mathbf{j}}_s^{\text{ZORA}}(\mathbf{r}', t), \quad (48)$$

where the paramagnetic, diamagnetic, and spin contributions to the current, $\hat{\mathbf{j}}_p^{\text{ZORA}}(\mathbf{r}', t)$, $\hat{\mathbf{j}}_d^{\text{ZORA}}(\mathbf{r}', t)$, and $\hat{\mathbf{j}}_s^{\text{ZORA}}(\mathbf{r}', t)$, respectively, are given by

$$\hat{\mathbf{j}}_p^{\text{ZORA}}(\mathbf{r}') = -\frac{i}{2} K(\mathbf{r}') [\delta(\mathbf{r}' - \mathbf{r}) \nabla - \nabla^\dagger \delta(\mathbf{r}' - \mathbf{r})], \quad (49)$$

$$\hat{\mathbf{j}}_d^{\text{ZORA}}(\mathbf{r}', t) = \frac{1}{c} K(\mathbf{r}') \delta(\mathbf{r}' - \mathbf{r}) \mathbf{A}_s(\mathbf{r}, t), \quad (50)$$

$$\hat{\mathbf{j}}_s^{\text{ZORA}}(\mathbf{r}') = K(\mathbf{r}') \nabla' \times \hat{\mathbf{s}}(\mathbf{r}'), \quad (51)$$

with

$$\hat{\mathbf{s}}(\mathbf{r}') = \frac{1}{2} \delta(\mathbf{r}' - \mathbf{r}) \boldsymbol{\sigma}. \quad (52)$$

It now becomes clear that the composition of the ZORA current density is similar to the one obtained in the Gordon decomposition of the Dirac current,^{2-4,41} except for an additional scaling factor $K(\mathbf{r}')$. Note that one arrives at the same expression [Eq. (48)] for the ZORA current operator by starting from the following anticommutator:

$$\hat{\mathbf{j}}^{\text{ZORA}}(\mathbf{r}') = \frac{1}{2} \{ \hat{\mathbf{v}}^{\text{ZORA}}, \delta(\mathbf{r}' - \mathbf{r}) \}, \quad (53)$$

with the zeroth order approximation of the mean velocity operator given as

$$\hat{\mathbf{v}}^{\text{ZORA}} = -i [\hat{\mathbf{r}}, \hat{h}^{\text{ZORA}}]. \quad (54)$$

This relation guarantees the validity of the Thomas-Reiche-Kuhn f -sum rule, which is used in the form of the approximate conductivity sum rule in our response calculations.³³ In a similar way one can show that the ZORA expressions for the density and current-density operators, Eqs. (46) and (48), satisfy the continuity equation,

$$\left(\frac{d\hat{\rho}}{dt} \right)^{\text{ZORA}}(\mathbf{r}, t) = -\nabla \cdot \hat{\mathbf{j}}^{\text{ZORA}}(\mathbf{r}, t). \quad (55)$$

C. Linear response formulation

As immediate application we can study relativistic effects in the time-dependent current-density formulation of the linear response of solids.³¹⁻³³ Here we will use the formalism in the zeroth order approximation. We consider a Kohn-Sham system in the ground state described by the stationary ZORA Hamiltonian,

$$\hat{H}_0^{\text{ZORA}} = \sum_i \hat{h}_0^{\text{ZORA}}(\mathbf{r}_i), \quad (56)$$

where $\hat{h}_0^{\text{ZORA}}(\mathbf{r})$ is the one-electron ground-state ZORA Hamiltonian,

$$\hat{h}_0^{\text{ZORA}}(\mathbf{r}) = v_{s,0}(\mathbf{r}) + \boldsymbol{\sigma} \cdot \mathbf{p} \frac{c^2}{2c^2 - v_0(\mathbf{r})} \boldsymbol{\sigma} \cdot \mathbf{p}. \quad (57)$$

We study the response of the system to small perturbing potentials $\delta v_s(\mathbf{r}, t)$ and $\delta \mathbf{A}_s(\mathbf{r}, t)$.^{31,33} The one-electron time-dependent ZORA Hamiltonian [Eq. (45)] can then be written as

$$\hat{h}^{\text{ZORA}}(\mathbf{r}, t) = \hat{h}_0^{\text{ZORA}}(\mathbf{r}) + \delta \hat{h}^{\text{ZORA}}(t), \quad (58)$$

where the perturbation $\delta \hat{h}^{\text{ZORA}}(t)$ is given by

$$\begin{aligned} \delta \hat{h}^{\text{ZORA}}(t) = \int \left(\hat{\rho}^{\text{ZORA}}(\mathbf{r}') \delta v_s(\mathbf{r}', t) + \frac{1}{c} (\hat{\mathbf{j}}_p^{\text{ZORA}}(\mathbf{r}') \right. \\ \left. + \hat{\mathbf{j}}_s^{\text{ZORA}}(\mathbf{r}')) \cdot \delta \mathbf{A}_s(\mathbf{r}', t) \right. \\ \left. + \frac{K(\mathbf{r}')}{2c^2} \hat{\rho}^{\text{ZORA}}(\mathbf{r}') \delta \mathbf{A}_s^2(\mathbf{r}', t) \right) d\mathbf{r}'. \end{aligned} \quad (59)$$

Note that the term involving $\hat{\mathbf{j}}_s^{\text{ZORA}}(\mathbf{r}')$ on the right-hand side of Eq. (59) contains the perturbation due to a magnetic field $\delta \mathbf{B}_s(\mathbf{r}, t) = \nabla \times \delta \mathbf{A}_s(\mathbf{r}, t)$,

$$\begin{aligned}
& \frac{1}{c} \int \hat{\mathbf{j}}_s^{\text{ZORA}}(\mathbf{r}') \cdot \delta \mathbf{A}_s(\mathbf{r}', t) d\mathbf{r}' \\
&= -\frac{1}{c} \int \hat{\mathbf{s}}(\mathbf{r}')(\mathbf{r}')(\nabla K(\mathbf{r}') \delta \mathbf{A}_s(\mathbf{r}', t)) d\mathbf{r}' \\
&\quad -\frac{1}{c} \int K(\mathbf{r}') \hat{\mathbf{s}}(\mathbf{r}')(\mathbf{r}') \cdot \delta \mathbf{B}_s(\mathbf{r}', t) d\mathbf{r}'. \quad (60)
\end{aligned}$$

We will not treat response to magnetic fields in this work, thus $\delta \mathbf{B}_s(\mathbf{r}', t) = 0$. Furthermore in Appendix B we show that for Coulomb-type potentials the remaining term in expression (60) gives a very small contribution to the perturbation [Eq. (59)].

It now becomes clear how we can solve the linear response for a Kohn-Sham system within the ZORA approximation. We first solve the time-independent ZORA equation [Eq. (56)] to obtain the ground-state orbitals and orbital energies. Given the perturbation [Eq. (59)], in which we retain only terms linear in the field, we can then evaluate the various response functions and solve self-consistently the equations describing the induced density and induced current density. In Appendix C we show that these two quantities can be expressed in an analogous way as in the nonrelativistic case³³ in terms of q -dependent Kohn-Sham response functions, which only involve the ground-state orbitals, orbital energies, and occupation numbers,

$$\begin{aligned}
\chi_{abq}(\mathbf{r}, \mathbf{r}', \omega) &= \frac{1}{N_k} \sum_k \sum_{ia} \frac{(f_{ik} - f_{ak+q})}{1 + \delta_{i,a}} \\
&\times \frac{\langle \Psi_{ik} | \hat{a}_q(\mathbf{r}) | \Psi_{ak+q} \rangle \langle \Psi_{ak+q} | \hat{b}_{-q}(\mathbf{r}') | \Psi_{ik} \rangle}{\epsilon_{ik} - \epsilon_{ak+q} + \omega + i\eta} \\
&+ \text{c.c.}(-\mathbf{q}, -\omega), \quad (61)
\end{aligned}$$

where the summation is over the (partially) occupied bands i , with occupation number $f_{ik} = 1$, and the unoccupied bands a , with occupation number $f_{ik} = 0$. The operators $\hat{a}_q(\mathbf{r})$ and $\hat{b}_q(\mathbf{r})$ can be either

$$\hat{\rho}_q(\mathbf{r}') = e^{-iq \cdot \mathbf{r}'} \delta(\mathbf{r}' - \mathbf{r}) \quad (62)$$

or

$$\begin{aligned}
\hat{\mathbf{j}}_q(\mathbf{r}') &= -\frac{i}{2} (\hat{\rho}_q(\mathbf{r}') K(\mathbf{r}') \nabla - \nabla^\dagger K(\mathbf{r}') \hat{\rho}_q(\mathbf{r}')) \\
&+ e^{-iq \cdot \mathbf{r}'} K(\mathbf{r}') \nabla' \times \hat{\mathbf{s}}(\mathbf{r}'). \quad (63)
\end{aligned}$$

The Bloch orbitals $\Psi_{ik}(\mathbf{r})$ are now two-component spinors and are solutions of the ground-state ZORA equation [Eq. (57)]. From the macroscopic induced current one can calculate the macroscopic dielectric function, which (at a wave vector $\mathbf{q} = 0$ and in the adiabatic local density approximation) can be defined as³³

$$\epsilon(\omega) = (1 + 4\pi\chi_e^{\text{inter}}(\omega)) - \frac{4\pi i}{\omega} \sigma^{\text{intra}}(\omega). \quad (64)$$

Here the term in bracket on the right-hand side represents the interband contribution to the dielectric function, while the other term is the intraband contribution. The former is due to

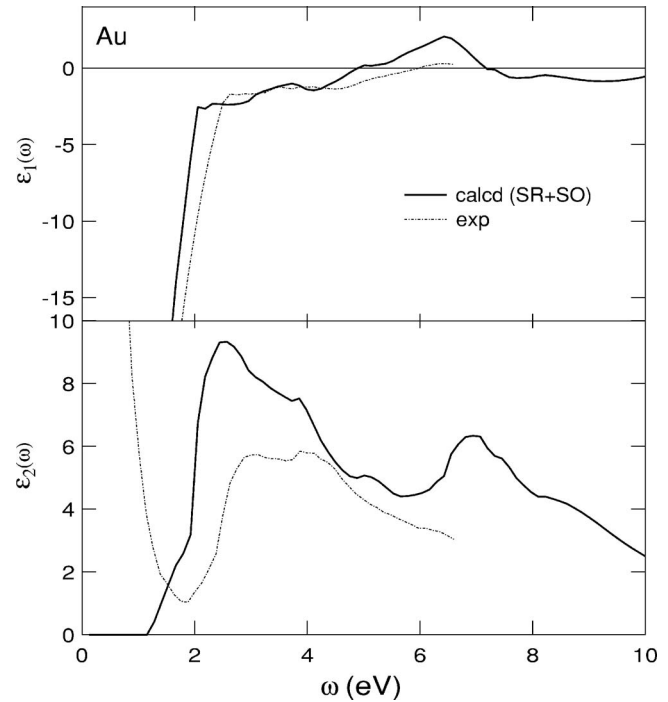


FIG. 1. Real (upper graph) and imaginary (lower graph) parts of the dielectric function of Au. The relativistic ZORA calculations (bold solid lines) are compared with experimental results (dotted-dashed lines) taken from Ref. 34.

transitions between occupied and unoccupied bands, while the latter is due to transitions within the same partially occupied bands. Clearly, these last transitions are not possible in nonmetallic systems, which are characterized by bands that are either fully occupied or fully unoccupied.

III. APPLICATIONS

To test our method we calculate the dielectric functions of the metals Au and W, the semiconductors ZnTe and CdTe, and the semimetal HgTe in the spectral range of 0–10 eV. In these systems spin-orbit effects are expected to be important: degeneracies at the Fermi level are lifted in W,²⁰ and the top valence bands are split in Au (Ref. 19) and in the zincblende-type nonmetals.^{25,26}

A. Computational details

We use the experimental lattice constants of 4.08 Å for Au in a fcc lattice, 3.16 Å for W in a bcc lattice, 6.09 Å for ZnTe, 6.48 Å for CdTe, and 6.48 Å for HgTe in a zincblende lattice. All calculations are performed using a modified version of the ADF-BAND program.^{31–33,42–44} We use a Slater-type orbital triple-zeta basis set augmented with two polarization functions. Cores are kept frozen up to 3p for Zn, 4p for Cd and Te, and 4f for Hg, Au, and W. We find converged results for the dielectric functions using 175 sample points in the irreducible wedge of the Brillouin zone, except in the relativistic calculations for W, for which we find converged results in the frequency range of 0–3 eV using 1771 sample points, and for CdTe and HgTe, where we use 1105 sample points. The static dielectric values are obtained for all systems by using 1105 sample points. For the semimetal

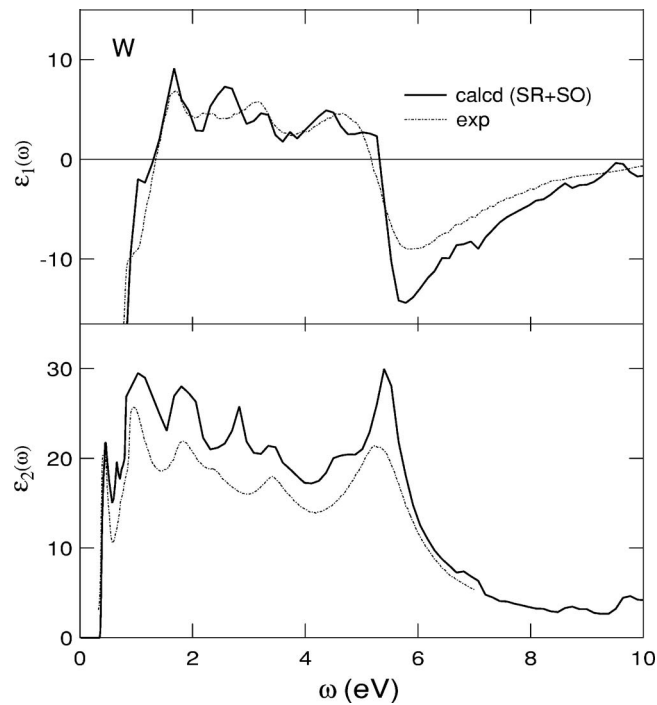


FIG. 2. Real (upper graph) and imaginary (lower graph) parts of the dielectric function of W. The relativistic ZORA calculations (bold solid lines) are compared with experimental results (dotted-dashed lines) taken from Ref. 35. To show the peak at 0.42 eV in the experimental absorption, we have reported only the interband contribution to the absorption, as extrapolated from experiments in Ref. 35.

HgTe we extrapolated this value from the linear relation found in the frequency range of 0.01–0.1 eV for the real part of the dielectric function versus ω^2 . In all our ground-state calculations we use the Vosko-Wilk-Nusair parametrization⁴⁵ of the local density approximation (LDA) exchange-correlation potential, which is also used to derive the adiabatic local density approximation of the exchange-correlation kernel for the response calculations. Additional computational details can be found in previous publications.^{19,20,33}

B. Metals: Au and W

We analyzed in detail the electronic band structures and optical properties of Au and W in previous works.^{19,20} In particular, we discussed the effect of the scalar relativistic corrections in the linear response of the two metals. Some deviations from experiments were attributed to the neglect of the spin-orbit coupling in the calculations. Based on the effect of spin-orbit coupling on the band structure, we argued that an improvement of the low-frequency onset of the interband transitions in the absorption of Au could be expected. Similarly in W a peaked onset around 0.60 eV could be expected, rather than a gapless interband absorption. The dielectric functions of Au and W calculated by including scalar and spin-orbit effects both in the ground state and response calculations are presented in Figs. 1 and 2. Treatment of spin orbit does not correct the overestimation of the height of the first peak and the redshift of the onset of the interband transitions that are obtained in the scalar relativistic calculations for Au.¹⁹ However, a small shoulder near the onset appears in

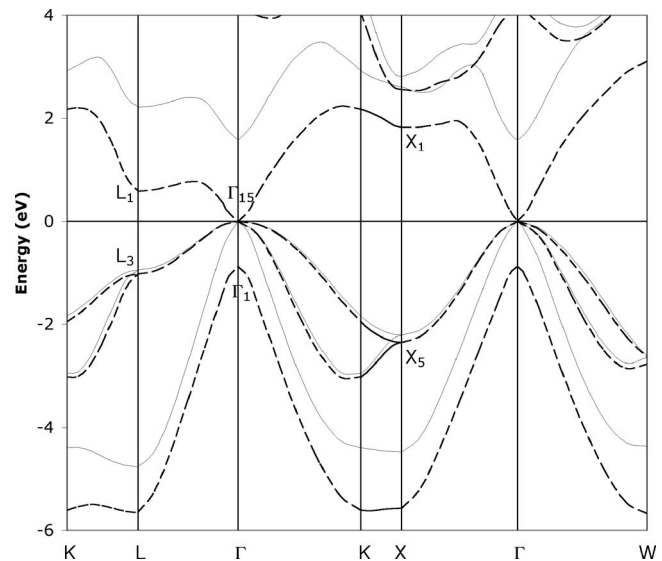


FIG. 3. Theoretical LDA ground-state band structures of HgTe. The thin lines refer to nonrelativistic calculations; the dashed lines refer to scalar relativistic ZORA calculations.

the spectrum, which is also present in the experimental spectrum. Spin-orbit coupling introduces a small finite gap in the interband absorption spectrum of W, which otherwise shows interband absorption approaching a constant value for frequencies below ≈ 0.5 eV.²⁰ To show the experimental onset of the interband absorption and the peak at 0.42 eV, we have reported in Fig. 2 the experimental interband absorption of W. This spectrum has been extrapolated by Weaver *et al.* by assuming a Drude behavior of the absorption in the infrared below 0.15 eV.³⁵ The rest of the theoretical spectrum remains similar to that one calculated by taking into account only scalar relativistic effects.²⁰ Both in Au and W the features in the absorption spectrum have a higher intensity in the calculations than what is observed experimentally. For these systems, treatment of spin-orbit coupling has significant effect on the spectra yielding extra features in agreement with experiments.

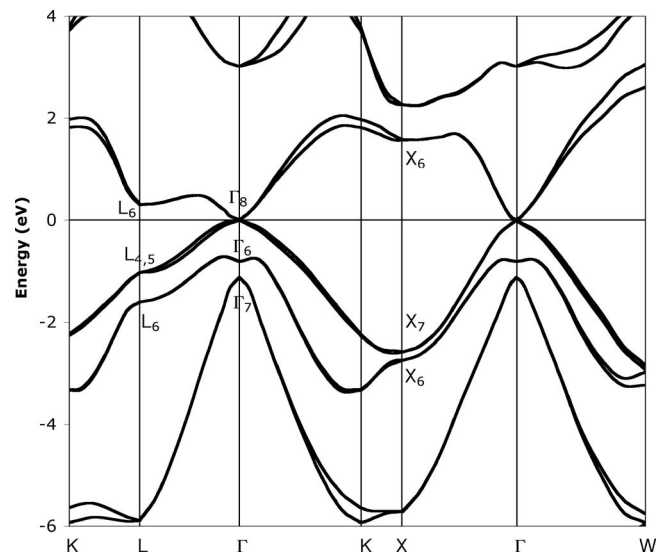


FIG. 4. ZORA relativistic LDA ground-state band structures of HgTe.

TABLE I. Calculated energy gaps ($\Gamma_8-\Gamma_6$ in the double-group representation) (eV) and spin-orbit splittings (eV) of valence bands at Γ ($\Gamma_7-\Gamma_8$) and L ($L_8-L_{4,5}$) for ZnTe, CdTe, and HgTe. The experiments are taken from Ref. 25.

		NR	SR	SR+SO	Expt. ^a
ZnTe	$\Gamma_8-\Gamma_6$	2.03	0.99	0.71	2.39
	$\Gamma_7-\Gamma_8$			0.93	0.91
	$L_8-L_{4,5}$			0.54	0.53
CdTe	$\Gamma_8-\Gamma_6$	1.62	0.45	0.18	1.59
	$\Gamma_7-\Gamma_8$			0.89	0.90
	$L_8-L_{4,5}$			0.54	0.54
HgTe	$\Gamma_8-\Gamma_6$	1.52	-0.88	-0.81	-0.30
	$\Gamma_7-\Gamma_8$			1.12	1.08
	$L_8-L_{4,5}$			0.57	0.62

^aData taken from Ref. 25.

C. Nonmetals: II-VI zinc-blende-type ZnTe, CdTe, HgTe

As expected, scalar relativistic effects shift the band energies with respect to the nonrelativistic results. In ZnTe and CdTe the dispersion of the valence and conduction bands is similar both in nonrelativistic and scalar relativistic band structures, thus nonrelativistic and scalar relativistic optical spectra can be expected to differ only in the energy position of the main spectral features. In contrast with these, in HgTe relativistic effects induce drastic changes in the electronic structure and, thus, in the optical properties: already the inclusion of scalar relativistic effects changes the character of this compound from semiconductor, as it appears to be in nonrelativistic calculations, to semimetal with an inverted band order. Indeed, as shown in Figs. 3 and 4, the s -like ($6s$ Hg) states at Γ_1 (Γ_6 in the double group representation) are stabilized more than the p -like ($5p$ Te) states at Γ_{15} (Γ_8 in the double group representation), resulting in a vanishing band

gap and an inversion of the typical band order.²⁷ The inclusion of spin-orbit coupling leads, in particular, to a splitting of several states in the three zinc-blende-type systems: L_3 (in the single group representation) splits into L_6 and $L_{4,5}$ (in the double group representations), Γ_{15} becomes Γ_7 and Γ_8 , and X_5 becomes X_6 and X_7 . Some of these splittings are well visible in the optical spectra as we will shortly show. In Table I we compare the nonrelativistic, scalar relativistic ZORA, and relativistic ZORA band gaps and spin-orbit splittings at Γ_{15} and L_3 with the observed values collected in Ref. 25 for ZnTe, CdTe, and HgTe. Inspection of this table reveals the well-known underestimation of the band gap in semiconductors by using the local density approximation. The inclusion of relativity decreases even more the band gap, with the relativistic band gaps being about 1.4–1.7 eV smaller than the experimental values. In HgTe relativity is essential to describe the negative band gap, which is, however, overestimated in the calculations with respect to the observed value. The main splittings that are visible in the spectra are well reproduced in our calculations. In Figs. 5–7 we have reported the calculated and measured^{23,28} real and imaginary parts of the dielectric functions for the three compounds. The features obtained in the nonrelativistic calculations of ZnTe and CdTe also appear in the scalar relativistic ZORA and relativistic ZORA calculations, but now at lower energies. In addition a doublet structure becomes visible in the relativistic ZORA calculations for ZnTe at about 2.7 eV and for CdTe at about 2.5 eV, which are also present in the experimental spectra but not in the scalar relativistic ZORA and in the nonrelativistic calculations. This is in line with the assignment of the doublet structure to the splittings at L_3 and along the Γ_{15} - L_3 line.^{22–24} The calculated spectra are, however, uniformly redshifted by about 0.6–0.9 eV with respect to the experimental curves. In particular, the relativistic ZORA spectra of CdTe show a low-frequency peak, which is too

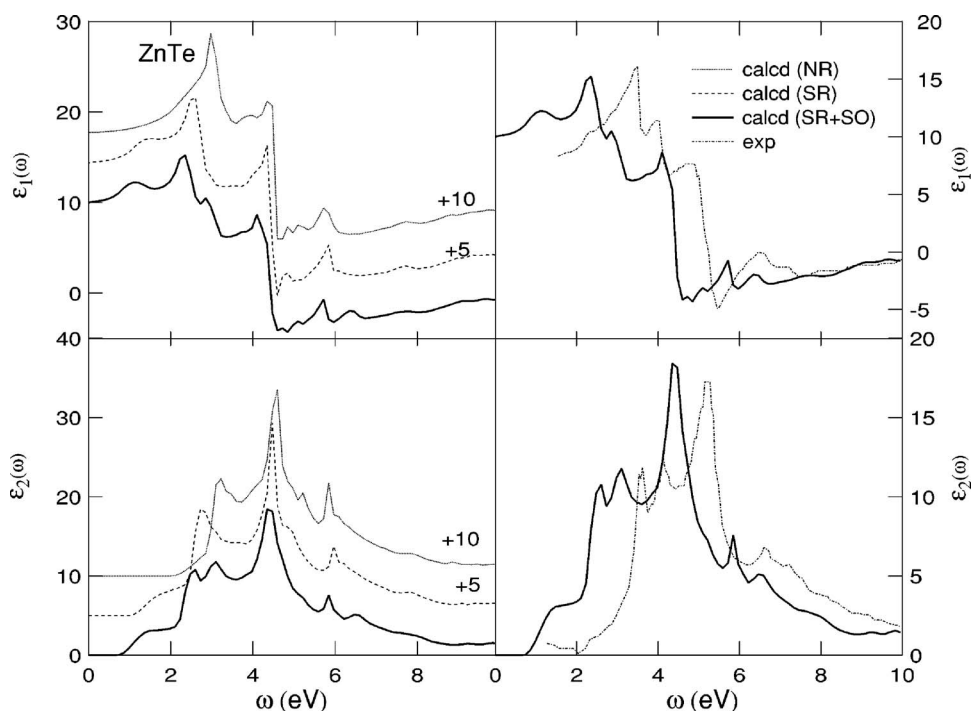


FIG. 5. Real (upper graph) and imaginary (lower graph) parts of the dielectric function of ZnTe. In the left panel we compare nonrelativistic calculations (thin lines), scalar relativistic ZORA calculations (dashed lines), and relativistic ZORA calculations (bold lines). To facilitate the comparison we have rigidly shifted upwards nonrelativistic ($\epsilon(\omega)+10$) and scalar relativistic ZORA ($\epsilon(\omega)+5$) curves. In the right panel we compare the relativistic ZORA calculations with the experiments (dotted-dashed lines) from Ref. 28.

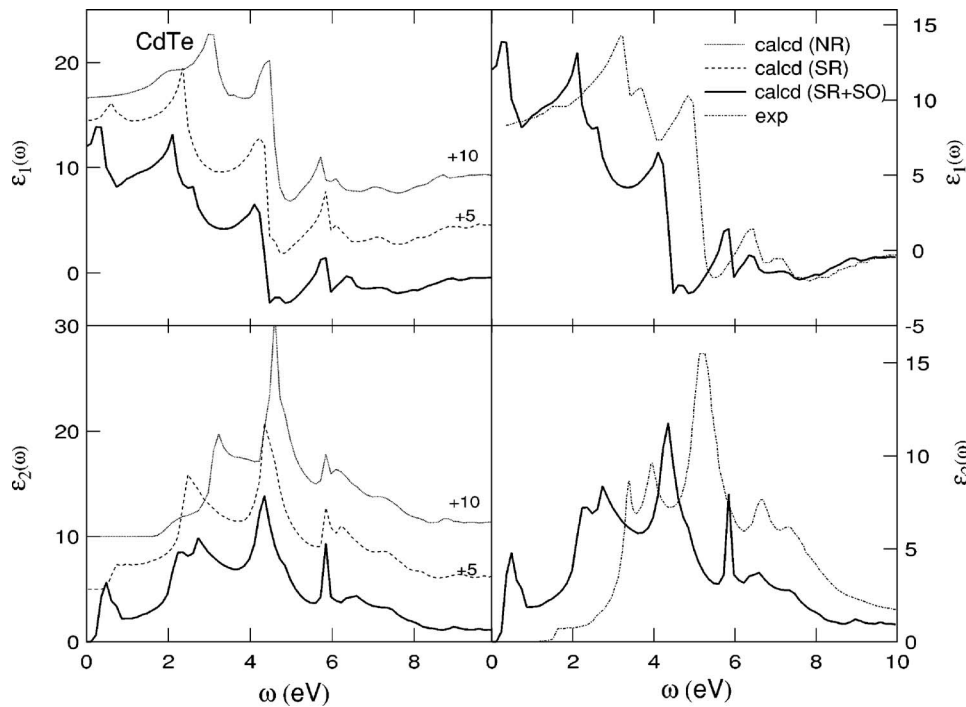


FIG. 6. Real (upper graph) and imaginary (lower graph) parts of the dielectric function of CdTe. In the left panel we compare nonrelativistic calculations (thin lines), scalar relativistic ZORA calculations (dashed lines), and relativistic ZORA calculations (bold lines). To facilitate the comparison we have rigidly shifted upwards nonrelativistic ($\epsilon(\omega)+10$) and scalar relativistic ZORA ($\epsilon(\omega)+5$) curves. In the right panel we compare the relativistic ZORA calculations with the experiments (dotted-dashed lines) from Ref. 28.

high as result of the too low frequency at which it occurs. Note that this redshift is compatible but smaller than the error in the calculated band gaps, in line with previous findings.^{17,32} Our results indicate that for ZnTe and CdTe the relative position of the *s*-like conduction band with respect to the *p*-like top valence band is too low, whereas the dispersion of the bands is well described. The spectra of HgTe reflect the strong impact of relativity on the electronic structure: in particular, the relativistic absorption spectra show the onset at $\hbar\omega=0$ eV, while the nonrelativistic one shows the onset at a finite frequency and is quite different from the experiments. In the relativistic ZORA spectra all the main

spectral features are present and reasonably well described in intensity, although they are redshifted with respect to the experimental curves by ~ 1 eV. An analogous redshift is also present in the scalar relativistic ZORA spectra. The calculated and measured^{29,30} static dielectric functions are reported in Table II. We find that in the two semiconductors the nonrelativistic results are in better agreement with the experiments than the relativistic ones. Scalar relativistic ZORA and relativistic ZORA calculations overestimate the dielectric constants, as direct consequence of the strong underestimation of the corresponding band gaps. For HgTe, instead, both nonrelativistic and relativistic results are quite different from

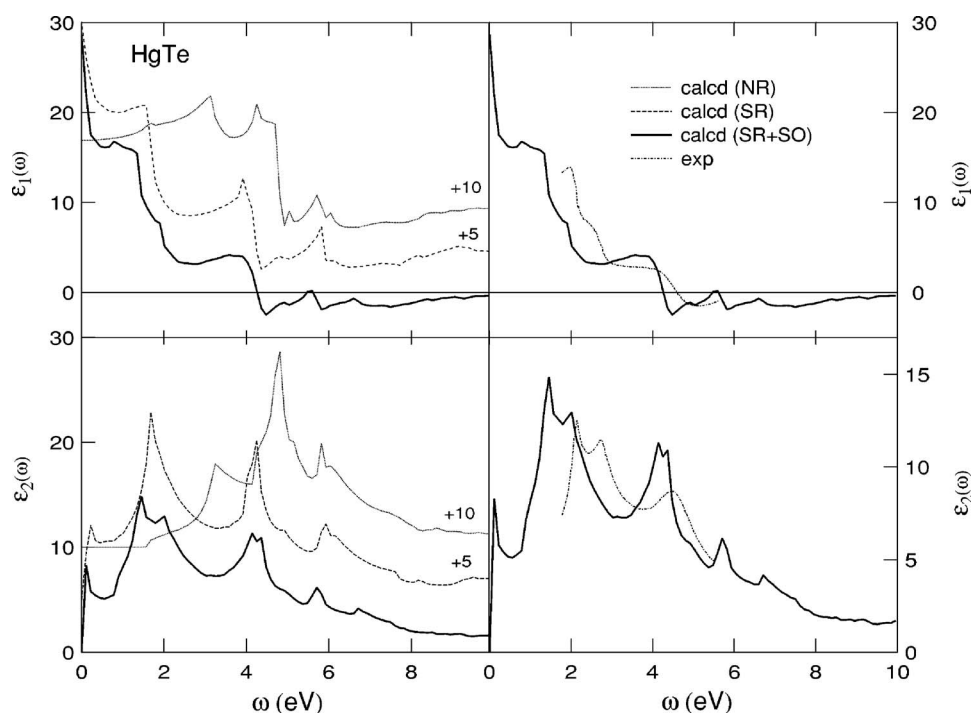


FIG. 7. Real (upper graph) and imaginary (lower graph) parts of the dielectric function of HgTe. In the left panel we compare nonrelativistic calculations (thin lines), scalar relativistic ZORA calculations (dashed lines), and relativistic ZORA calculations (bold lines). To facilitate the comparison we have rigidly shifted upwards nonrelativistic ($\epsilon(\omega)+10$) and scalar relativistic ZORA ($\epsilon(\omega)+5$) curves. In the right panel we compare the relativistic ZORA calculations with the experiments (dotted-dashed lines) from Ref. 23.

TABLE II. Nonrelativistic, scalar relativistic ZORA, and relativistic ZORA dielectric constants (eV) calculated for ZnTe, CdTe, and HgTe. The experiments are taken from Refs. 29 and 30.

	ZnTe	CdTe	HgTe
NR	7.72	6.63	6.90
SR	9.22	9.56	24.00
SR+SO	9.70	13.07	28.71
Expt. ^a	7.28	7.21	14.0 ^{3b}

^aDielectric constants taken from Refs. 29 and 30.

^bThis value is taken from Ref. 30 as the sum $\epsilon_{\infty} + \Delta\epsilon'_{\text{inter}}$ at room temperature.

the experimental value at 300 K. However, our relativistic results are not necessarily in contradiction with the experiments, as the experimental value depends strongly on the temperature and should increase at lower temperatures.³⁰

IV. CONCLUSIONS

In this paper we derived a relativistic two-component formulation of time-dependent current-density-functional theory following the formulation for the ground state proposed by van Lenthe *et al.*^{8,9} In order to achieve this we applied a Foldy-Wouthuysen transformation to the time-dependent Dirac-Kohn-Sham equations of relativistic density functional theory. In the derivation three series expansions are involved: an expansion for the Foldy-Wouthuysen transformation, one for the two-component Hamiltonian, and one for the two-component operators. The two-component Hamiltonian is Hermitian and gauge invariant at each order of approximation with respect to the gauge of the electromagnetic field. This allows for physical acceptable approximations at arbitrary order. We showed that to zeroth order in the expansion of the Foldy-Wouthuysen transformation, the series expansion of the Hamiltonian, truncates at zeroth order exactly. This result allows us to truncate the expansion for the density and current-density operators at lowest order while retaining the validity of the continuity equation. To zeroth order the density operator has the same expression as in the nonrelativistic case, whereas the current-density operator has a paramagnetic, a diamagnetic, and a spin contribution, similar to the Gordon decomposition of the Dirac current operator. By combining the time-dependent zeroth order formalism with the TDCDFT formulation of the linear response of extended systems, we obtained a method which can treat in a unified way the orbital and spin contributions to the response to an electromagnetic field. As immediate application of the method we treated relativistic effects, including spin-orbit coupling, in the linear response of several metals and nonmetals. We showed that the main splittings in the band structures and in the optical spectra that are due to spin-orbit coupling are well described. However, band gaps remain underestimated and spectra redshifted with respect to the experimental results. These deviations are the result of an incorrect relative position of the valence and conduction bands, which is a shortcoming of LDA used in the ground-state description.

APPENDIX A: HERMITICITY OF THE TIME-DEPENDENT RELATIVISTIC TWO-COMPONENT HAMILTONIAN

We prove that the time-dependent two-component Schrödinger Hamiltonian [Eq. (38)] is Hermitian. To do this we show that the remainder \hat{Y} is Hermitian, where \hat{Y} is given by

$$\begin{aligned} \hat{Y} = & \frac{1}{2}(c\boldsymbol{\sigma} \cdot \boldsymbol{\pi} \hat{X} - \hat{X}^\dagger c\boldsymbol{\sigma} \cdot \boldsymbol{\pi}) \\ & - \sum_{n=1}^{\infty} a_n \sum_{m=0}^{n-1} (\hat{X}^\dagger \hat{X})^{n-m-1} (c\boldsymbol{\sigma} \cdot \boldsymbol{\pi} \hat{X} - \hat{X}^\dagger c\boldsymbol{\sigma} \cdot \boldsymbol{\pi}) \\ & \times (\hat{X}^\dagger \hat{X})^m \times \sqrt{1 + \hat{X}^\dagger \hat{X}}. \end{aligned} \quad (\text{A1})$$

If we consider $\sqrt{1 + \hat{X}^\dagger \hat{X}} = \sum_k a_k (\hat{X}^\dagger \hat{X})^k$, then we have

$$\begin{aligned} \hat{Y} = & \sum_{n,k} \left(a_n a_k - \frac{1}{2} \delta_{n1} \delta_{k0} \right) \sum_{m=0}^{n-1} (\hat{X}^\dagger \hat{X})^{n-m-1} (\hat{X}^\dagger c\boldsymbol{\sigma} \cdot \boldsymbol{\pi} \\ & - c\boldsymbol{\sigma} \cdot \boldsymbol{\pi} \hat{X}) (\hat{X}^\dagger \hat{X})^{m+k}. \end{aligned}$$

By introducing $p = n - m - 1 \geq 0$ and $q = m + k$ with $m \geq 0$, we can rewrite

$$\begin{aligned} \hat{Y} = & \sum_{p,q} \sum_{m=0}^q \left(a_{p+m+1} a_{q-m} - \frac{1}{2} \delta_{p0} \delta_{q0} \right) (\hat{X}^\dagger \hat{X})^p (\hat{X}^\dagger c\boldsymbol{\sigma} \cdot \boldsymbol{\pi} \\ & - c\boldsymbol{\sigma} \cdot \boldsymbol{\pi} \hat{X}) (\hat{X}^\dagger \hat{X})^q, \end{aligned}$$

which allows us to define the expansion coefficients,

$$c_{pq} = \sum_{m=0}^q a_{p+m+1} a_{q-m} - \frac{1}{2} \delta_{p0} \delta_{q0}. \quad (\text{A2})$$

We will now investigate some properties of these coefficients. Consider therefore the relation

$$(\sqrt{1 + \hat{X}^\dagger \hat{X}})^2 = \sum_{n,m} a_n a_m (\hat{X}^\dagger \hat{X})^{n+m} = 1 + \hat{X}^\dagger \hat{X}, \quad (\text{A3})$$

from which it follows that

$$\sum_{n=0}^k a_{k-n} a_n = \delta_{k0} + \delta_{k1}. \quad (\text{A4})$$

We can now prove that $c_{pq} = -c_{qp}$. We first write

$$c_{pq} = \sum_{m'=0}^q a_{(p+q+1)-m'} a_{m'} - \frac{1}{2} \delta_{p0} \delta_{q0},$$

where $m' = q - m$. We can now use relation (A4) in which $p + q + 1$ has the minimum value of one for $p = q = 0$, and hence

$$\begin{aligned} c_{pq} = & \delta_{p+q+1,0} + \delta_{p+q+1,1} - \sum_{m'=q+1}^{p+q+1} a_{(p+q+1)-m'} a_{m'} - \frac{1}{2} \delta_{p0} \delta_{q0} \\ = & \frac{1}{2} \delta_{p0} \delta_{q0} - \sum_{m''=0}^p a_{p-m''} a_{q+1+m''} = -c_{qp}, \end{aligned}$$

where $m'' = m' - q - 1$. We can then conclude that $\hat{Y}^\dagger = \hat{Y}$.

Moreover, all diagonal elements $c_{pp}=0$ and, in particular, $c_{00}=0$. As result \hat{Y} is of first order in $(\hat{X}^\dagger\hat{X})$.

APPENDIX B: THE TERM $\nabla K(\mathbf{r})$

For a Coulomb-type potential [e.g., $v_0(\mathbf{r})=-Z/r$] it follows that $K(\mathbf{r})\approx 1$ and $\nabla v_0(\mathbf{r})\ll 2c^2$ everywhere except close to the nucleus. The term $\nabla K(\mathbf{r})=K^2(\mathbf{r})\nabla v_0(\mathbf{r})/(2c^2)$ is thus smaller than 1 everywhere, except close to the nucleus. However, although there $\nabla K(\mathbf{r})$ can be quite large ($\sim 2c^2/Z$), the volume Ω where this happens is so small that the integrals where the term $\nabla K(\mathbf{r})$ appears are still of the order of Z^2/c^4 . This becomes clear if we consider only contributions to the integral from a small spherical volume of radius $Z/2c^2$, where $\nabla K(\mathbf{r})\approx 2c^2/Z$,

$$\int_{\Omega} |\nabla K(\mathbf{r})| F(\mathbf{r}) d\mathbf{r} \approx |\nabla K(\mathbf{0})| F(\mathbf{0}) \frac{4\pi}{3} \left(\frac{Z}{2c^2}\right)^3 \approx F(\mathbf{0}) \frac{4\pi}{3} \frac{Z^2}{4c^4}. \quad (\text{B1})$$

Here we have assumed that the function $F(\mathbf{r})\approx F(\mathbf{0})$ in the small volume Ω .

APPENDIX C: SYMMETRY OF THE RESPONSE FUNCTIONS IN THE PRESENCE OF SPIN

In Appendix A of Ref. 33 the equations describing the induced density and current density are derived by using time-reversal symmetry for the ground state. In the presence of magnetic fields the time-reversal symmetry is broken. In our case no magnetic fields are present in the ground state. For the spinless case the time-reversal operator K_0 is the complex conjugation combined with the inversion in the reciprocal space,

$$K_0 \psi_{n\mathbf{k}} = \psi_{n-\mathbf{k}}^*. \quad (\text{C1})$$

In the presence of spin the time-reversal operator becomes $K=UK_0$, with $U=i\sigma_y$ unitary. Thus two-component spinors $\Psi_{n\mathbf{k}}$ transform according to

$$K\Psi_{n\mathbf{k}} = i\sigma_y \Psi_{n-\mathbf{k}}^*, \quad (\text{C2})$$

and observables \hat{B} transform according to

$$K\hat{B}K^{-1} = U\hat{B}^*U^\dagger. \quad (\text{C3})$$

In particular, for the density and the current-density operators $\hat{\rho}_{\mathbf{q}}$ and $\hat{\mathbf{j}}_{\mathbf{q}}$ [given in Eqs. (62) and (63)], we have

$$K\hat{\rho}_{\mathbf{q}}K^{-1} = \hat{\rho}_{-\mathbf{q}} \quad (\text{C4})$$

$$K\hat{\mathbf{j}}_{\mathbf{q}}K^{-1} = -\hat{\mathbf{j}}_{-\mathbf{q}}. \quad (\text{C5})$$

By using these relations one can derive the equations for the induced density and current density in the presence of spin in an analogous way as in the spinless case [Eqs. (18) and (28) in Ref. 33].

¹See, for example, S. A. Wolf, D. D. Awschalom, R. A. Buhrman, J. M. Daughton, S. von Molnár, M. L. Roukes, A. Y. Chtchelkanova, and D. M.

- Treger, Science **294**, 1488 (2001).
²A. K. Rajagopal and J. Callaway, Phys. Rev. B **7**, 1912 (1973).
³E. Engel and M. R. Dreizler, in *Density Functional Theory II*, edited by R. F. Nalewajski, Topics in Current Chemistry Vol. 181 (Springer, Berlin, 1996), p. 1.
⁴E. Engel, in *Relativistic Electronic Structure Theory, Part I. Fundamentals*, edited by P. Schwerdtfeger (Elsevier, Amsterdam, 2002), p. 523.
⁵A. K. Rajagopal, J. Phys. C **11**, L943 (1978).
⁶A. H. MacDonald and S. H. Vosko, J. Phys. C **12**, 2977 (1979).
⁷L. L. Foldy and S. A. Wouthuysen, Phys. Rev. **78**, 29 (1950).
⁸E. van Lenthe, E. J. Baerends, and J. G. Snijders, J. Chem. Phys. **99**, 4597 (1993).
⁹E. van Lenthe, E. J. Baerends, and J. G. Snijders, J. Chem. Phys. **101**, 9783 (1994).
¹⁰M. Reher and A. Wolf, J. Chem. Phys. **121**, 2037 (2004).
¹¹J.-L. Heully, I. Lindgren, E. Lindroth, S. Lundqvist, and A.-M. Mårtensson-Pendrill, J. Phys. B **19**, 2799 (1986).
¹²Ch. Chang, M. Pellisier, and Ph. Durand, Phys. Scr. **34**, 394 (1986).
¹³F. Wang, T. Ziegler, E. van Lenthe, S. van Gisbergen, and E. J. Baerends, J. Chem. Phys. **122**, 204103 (2005).
¹⁴F. Wang and T. Ziegler, J. Chem. Phys. **123**, 194102 (2005).
¹⁵F. Wang and T. Ziegler, J. Chem. Phys. **123**, 154102 (2005).
¹⁶D. Peng, W. Zou, and W. Liu, J. Chem. Phys. **123**, 144101 (2005).
¹⁷F. Kootstra, P. L. de Boeij, H. Aissa, and J. G. Snijders, J. Chem. Phys. **114**, 1860 (2001).
¹⁸P. L. de Boeij, F. Kootstra, and J. G. Snijders, Int. J. Quantum Chem. **85**, 449 (2001).
¹⁹P. Romaniello and P. L. de Boeij, J. Chem. Phys. **122**, 164303 (2005).
²⁰P. Romaniello and P. L. de Boeij, Phys. Rev. B **73**, 075115 (2006).
²¹S. H. Groves, R. N. Brown, and C. R. Pidgeon, Phys. Rev. **161**, 779 (1967).
²²M. Cardona and D. L. Greenaway, Phys. Rev. **131**, 98 (1963).
²³L. Vinã, C. Umbach, M. Cardona, and L. Vodopyanov, Phys. Rev. B **29**, 6752 (1984).
²⁴D. J. Chadi, J. P. Walter, M. I. Cohen, Y. Petroff, and M. Balkanski, Phys. Rev. B **5**, 3058 (1972).
²⁵S.-H. Wei and A. Zunger, Phys. Rev. B **37**, 8958 (1988).
²⁶See, for example, M. Cardona, K. L. Shaklee, and F. H. Pollak, Phys. Rev. **154**, 696 (1967).
²⁷S. H. Groves and W. Paul, *Proceedings of the Seventh International Conference on Semiconductors* (Academic, New York, 1965).
²⁸J. L. Freilouf, Phys. Rev. B **7**, 3810 (1973).
²⁹D. T. F. Marple, J. Appl. Phys. **35**, 539 (1964).
³⁰M. Grynberg, R. le Toullec, and M. Balkanski, Phys. Rev. B **9**, 517 (1974).
³¹F. Kootstra, P. L. de Boeij, and J. G. Snijders, J. Chem. Phys. **112**, 6517 (2000).
³²F. Kootstra, P. L. de Boeij, and J. G. Snijders, Phys. Rev. B **62**, 7071 (2000).
³³P. Romaniello and P. L. de Boeij, Phys. Rev. B **71**, 155108 (2005).
³⁴P. B. Johnson and R. W. Christy, Phys. Rev. B **9**, 5056 (1974).
³⁵J. H. Weaver, C. G. Olson, and D. W. Lynch, Phys. Rev. B **12**, 1293 (1975).
³⁶O. L. Brill and B. Goodman, Am. J. Phys. **35**, 832 (1967).
³⁷A. K. Rajagopal, Phys. Rev. A **50**, 3759 (1994).
³⁸W. Kutzelnigg and W. Liu, Mol. Phys. **104**, 2225 (2006).
³⁹R. E. Moss, *Advanced Molecular Quantum Mechanics* (Chapman and Hall, London, 1973).
⁴⁰E. J. Baerends, W. H. E. Schwarz, P. Schwerdtfeger, and J. G. Snijders, J. Phys. B **23**, 3225 (1990).
⁴¹P. Romaniello, Ph.D. thesis, University of Groningen, 2006; <http://dissertations.ub.rug.nl/faculties/science/2006/p.romaniello>
⁴²G. te Velde and E. J. Baerends, Phys. Rev. B **44**, 7888 (1991); J. Comput. Phys. **99**, 84 (1992).
⁴³C. Fonseca Guerra, O. Visser, J. G. Snijders, G. te Velde, and E. J. Baerends, in *Methods and Techniques in Computational Chemistry*, edited by E. Clementi and G. Corongiu (STEF, Cagliari, 1995), p. 305.
⁴⁴G. te Velde, F. M. Bickelhaupt, E. J. Baerends, C. Fonseca Guerra, S. J. A. van Gisbergen, J. G. Snijders, and T. Ziegler, J. Comput. Chem. **22**, 931 (2001).
⁴⁵S. H. Vosko, L. Wilk, and M. Nusair, Can. J. Phys. **58**, 1200 (1980).